ChemComm

COMMUNICATION

View Article Online
View Journal | View Issue

Cite this: *Chem. Commun.*, 2019, 55, 1782

Received 30th November 2018,
Accepted 10th January 2019

DOI: 10.1039/c8cc09517e

rsc.li/chemcomm

Real-time visualization of autophagy by monitoring the fluctuation of lysosomal pH with a ratiometric two-photon fluorescent probe†

Peng Ning,‡[a] Liling Hou,‡[a] Yan Feng,*[a] Guoyong Xu,[b] Yuyuan Bai,[a] Haizhu Yu[a] and Xiangming Meng*[ab]

A benzimidazole-decorated two-photon fluorescent probe (Lyso-MPCB) based on the *p*-methoxyphenylacetylene-substituted carbazole was developed for detecting lysosomal pH with a double-channel signal, which can be used to visualize autophagy by real-time imaging the fluctuation of the pH in the lysosomes.

Autophagy is a lysosome-dependent degradation pathway for recycling misfolded proteins and dysfunctional organelles as well as providing nutrients during starvation.[1] Several conventional methods have been used to monitor such metabolic processes, including transmission electron microscopy (TEM), western blotting (Atg8/LC3), and GFP-Atg8/LC3 fluorescence microscopy.[2] Nevertheless, it's difficult to achieve real-time, rapid and low-cost visualization of autophagy in living cells by employing the above methods. Therefore, real-time detection of autophagy efficiently and economically is still a challenge.

In general, a lysosome and an autophagosome can be fused to generate an autolysosome during the membrane fusion process of autophagy.[3] The microenvironments (including polarity, pH, and viscosity, *etc.*) would fluctuate owing to the difference between the lysosome and autophagosome in this process.[4] Accordingly, it is feasible to monitor autophagy by detecting the microenvironmental variation, especially the pH, in a real-time fashion, which is the vital factor for the activity of acid hydrolases.[5] To date, a few small-molecule fluorescent probes have been reported for autophagy detection by responding to the changes in pH value.[6] However, the existing probes yield fluctuation of the emission intensity at a single particular wavelength. Such a turn-on type probe is liable to uneven probe loading and photobleaching. These limitations can be improved and simplified by developing one novel ratiometric pH fluorescent probe for autophagy detection. Ratiometric fluorescent probes can overcome several problems including local concentrations of probes, photobleaching and variations of the instrument, which can inhibit the quantitative and accurate determination of the analyte.[7] In addition, our reported studies have evidenced that the two-photon (TP) fluorescence performance of probes could enhance the spatial resolution in autophagy detection.[8] Therefore, it is of pressing need to design a TP ratiometric fluorescent probe to visualize autophagy by ratiometric imaging of the lysosomal pH fluctuation.

Here, we report a novel pH-sensitive TP ratiometric fluorescent probe (**Lyso-MPCB**) on the basis of *p*-methoxyphenylacetylene-substituted carbazole, an effective TP fluorophore reported in our previous work.[8c] The benzimidazole group in **Lyso-MPCB** was employed to respond to changes in pH with an obvious emission shift (65 nm). In addition, **Lyso-MPCB** was configured with the lysosome-locating group, morpholine.[9] This probe can specifically respond to changes in lysosomal pH and has good biocompatibility. To our knowledge, **Lyso-MPCB** was the first ratiometric small-molecule TP fluorescent probe to visualize autophagy by real-time imaging of the lysosomal pH fluctuation (Scheme 1). The synthetic route and detailed characterizations of **Lyso-MPCB** are shown in the ESI† (Scheme S1 and Fig. S11–S21).

Firstly, the pH-responsive profile of **Lyso-MPCB** was studied spectroscopically in Britton–Robinson (B–R) buffer (10 μM, 30% DMSO, v/v). Under basic conditions (pH = 8.2), the UV-Vis spectrum showed the maximum absorption peak at 340 nm (Fig. S1a, ESI†). With the pH value decreasing from 8.2 to 3.2, the peak at 340 nm was reduced gradually along with the emergence of a new peak at 385 nm. The nonlinear pH titration curve was established by plotting the ratio (A_{340nm}/A_{385nm}) of absorbance against pH value from 3.2 to 8.2 according to the Henderson–Hasselbalch equation[10] and good linearity was presented in a narrow acidic

[a] *School of Chemistry and Chemical Engineering, Center for Atomic Engineering of Advanced Materials, and Anhui Province Key Laboratory of Chemistry for Inorganic/Organic Hybrid Functionalized Materials, Anhui University, Hefei, Anhui 230601, China. E-mail: fy70@163.com, mengxm@ahu.edu.cn; Fax: +86 551 63861467; Tel: +86 551 63861467*

[b] *Institute of Physical Science and Information Technology, Anhui University, Hefei 230601, P. R. China*

† Electronic supplementary information (ESI) available: Experimental section, UV-Vis spectra, ^{1}H-NMR titration, selectivity experiment, theoretical calculations, cytotoxicity assay, colocalization experiments, western blotting, HRMS and NMR spectra. See DOI: 10.1039/c8cc09517e

‡ Both authors contributed equally to this work.

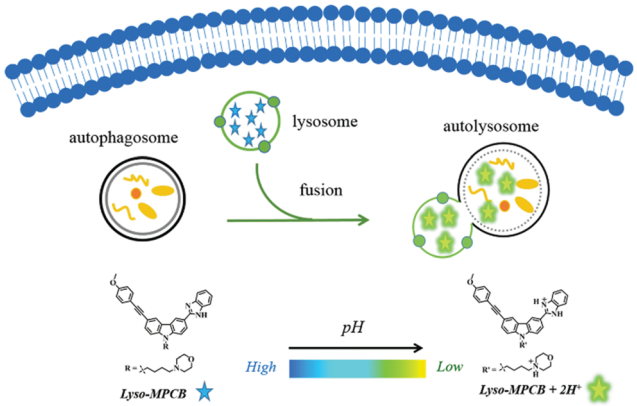

Scheme 1 Illustration of real-time visualization of autophagy with a double-channel signal using probe **Lyso-MPCB** in cells.

pH range (pH = 4.6–6.2) (Fig. S1b, ESI†). The isosbestic point at 370 nm indicated the protonation of **Lyso-MPCB**. As shown in Fig. 1a, the fluorescence emission spectra of **Lyso-MPCB** were tested in the pH range from 9.6 to 3.2. Under basic conditions (pH = 9.6), **Lyso-MPCB** exhibited weak blue fluorescence emission at 410 nm. When the pH decreased from 9.6 to 3.2, the evident green fluorescence emission at 475 nm was gradually increased with a large red-shift of 65 nm. The ratios (I_{475nm}/I_{410nm}) of fluorescence intensity displayed apparent enlargement from 0.34 to 47.62 (~140-fold enhancements) along with the enlarged fluorescence quantum yield from 5.23% to 11.27%. These results indicated that **Lyso-MPCB** was highly sensitive to changes in pH *in vitro*. Moreover, the pK_a value was obtained to be 4.86 fitted by the Henderson–Hasselbalch equation (eqn (S1), ESI†).[5b,10] Such lower pK_a value was suitable for determining the changes in pH in the lysosomal range (4.5–5.5).[11]

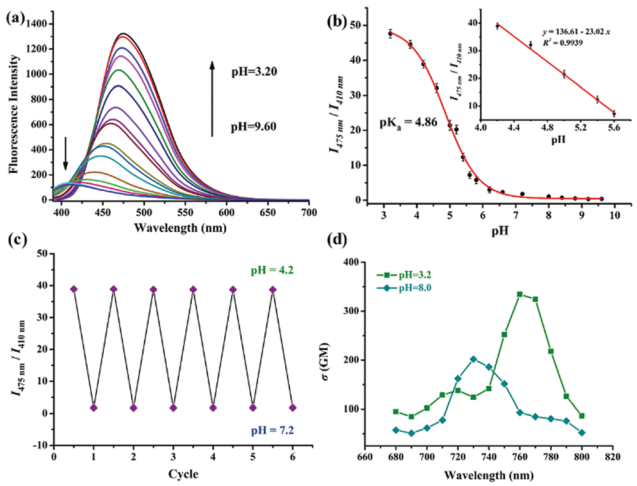

Fig. 1 (a) Emission spectra of **Lyso-MPCB** (10 μM) in B–R buffer solution with different pH from 9.60 to 3.20 (with 30% DMSO, λ_{ex} = 370 nm). (b) Plot of the fluorescence intensity ratio (I_{475nm}/I_{410nm}) *vs.* pH. Inset: Linear relationship of pH-dependent fluorescence intensity ratio (I_{475nm}/I_{410nm}). R^2 = 0.9939. (c) pH reversibility of **Lyso-MPCB** in B–R buffer solution (pH = 4.20 and 7.20). (d) Two-photon absorption cross-section of **Lyso-MPCB** with pH = 3.2 and 8.0, respectively. (λ_{ex} = 680–800 nm).

More importantly, the ratio signals (I_{475nm}/I_{410nm}) of **Lyso-MPCB** displayed a good linear relationship with pH values ranging from 4.2 to 5.6 (inset of Fig. 1b), which demonstrated that the probe can be an efficient tool for detecting the lysosomal pH change quantitatively.

^{1}H NMR titration experiments using DCl (deuterium chloride) in DMSO-d_6 were conducted to confirm the sensing mechanism of **Lyso-MPCB** for acid pH (Fig. S2, ESI†).[12] Compared with H1–H4 of the benzimidazole moiety in **Lyso-MPCB**, the corresponding four protons (H1′–H4′) of **Lyso-MPCB** + 2H$^+$ obviously shifted downfield due to the protonation of the nitrogen atom in the benzimidazole unit (H1 shifted 0.27 ppm, H4 shifted 0.15 ppm and H2, H3 shifted 0.35 ppm, respectively). Moreover, the time-dependent density functional theory (TD-DFT) calculations were employed to study the photophysical properties of **Lyso-MPCB** and its protonated configuration **Lyso-MPCB** + 2H$^+$.[13] As shown in Fig. S3 (ESI†), electrons were totally localized over the molecular skeleton at the ground and excited states of **Lyso-MPCB**, respectively. When probe **Lyso-MPCB** reacted with H$^+$, electrons were changed to distribute on the *p*-methoxyphenylacetylene-substituted carbazole unit as the donor group at the ground state, while the protonated benzimidazole unit as the acceptor group at the excited state of **Lyso-MPCB** + 2H$^+$, indicating an enhanced ICT process. The HOMO–LUMO gap value of **Lyso-MPCB** is larger than that of **Lyso-MPCB** + 2H$^+$ (3.92 eV *vs.* 2.10 eV), which is consistent with the hypochromic shift (from 340 nm to 385 nm) of the absorption spectra. It's clear that the enhancement of the ICT process in **Lyso-MPCB** + 2H$^+$ was caused by H$^+$-binding of the =N-atom in the benzimidazole group of **Lyso-MPCB**, showing that the probe is indeed pH-dependent.

In addition, the reversible response to pH between 4.2 and 7.2 of **Lyso-MPCB** was conducted in B–R buffer solution (with 30% DMSO) (Fig. 1c). The results distinctly showed that the process was fully reversible for at least 6 cycles, which indicated that **Lyso-MPCB** was sensitive and stable for pH detection between the protonation and deprotonation processes. Two-photon (TP) absorption properties of unprotonated and protonated **Lyso-MPCB** were carried out (Fig. 1d).[14] The maximum TP absorption cross-section value (δ) was 202 GM at 730 nm for the former and 340 GM at 760 nm for the latter, which attested that the protonated probe possessed a better two-photon absorption performance than that of the unprotonated one due to the enhanced ICT. Besides, **Lyso-MPCB** displayed no response to other analytes (amino acids and ions), showing that it's an excellent pH-dependent TP fluorescent probe with high selectivity (Fig. S4, ESI†). The time-dependent fluorescence response results of **Lyso-MPCB** in B–R buffer (pH = 5.0, with 30% DMSO) indicated that the ratios were stabilized at 2 min. These data fitted well to a monoexponential model and a first-order kinetic rate constant can be recovered as 0.0307 s^{-1} (R^2 = 0.99835) in this kinetic experiment (Fig. S5, ESI†).[15]

The cytotoxicity of probe **Lyso-MPCB** was tested by MTT assay before biological imaging, and the results indicated that the cell survival was as high as 89% even when the concentration of **Lyso-MPCB** reached 15 μM (Fig. S6, ESI†). Therefore, the probe was capable of biological imaging in living MCF-7

cells as expected. Its specificity of localizing lysosomes was carried out in MCF-7 cells *via* colocalization fluorescence imaging technology. As shown in Fig. S7 (ESI†), probe **Lyso-MPCB** and LysoTracker Red overlapped very well, and the Pearson's colocalization coefficient (R) was found to reach 0.935. On the contrary, the Pearson's colocalization coefficient between **Lyso-MPCB** and MitoTracker Red was only 0.336 in MCF-7 cells. Hence, these results demonstrated that our probe could localize to the lysosome perfectly and could be utilized as a reliable tool for further investigations in lysosomal regions.

Subsequently, we verified the capability of probe **Lyso-MPCB** to quantify the intracellular pH in a ratiometric manner in living cells. The intracellular pH of MCF-7 cells was well-distributed by using the high K^+ buffer (0.5 mM $MgSO_4$, 1 mM $CaCl_2$, 1 mM NaH_2PO_4, 5 mM glucose, 30 mM NaCl, 120 mM KCl, and 20 mM HEPES) with 10 mM nigericin at different pH values (3.0–8.0).[5c,9a] The blue channel exhibited a continual increase along with a gradual decrease in the green fluorescence when the intracellular pH values enhanced from 3.0 to 8.0 (Fig. 2a). Similarly, obvious remarkable pseudocolor changes were observed in the pH range 3.0–8.0. Meanwhile, the ratio images (I_{green}/I_{blue}) displayed a pH-dependent characteristic greatly from pH 3.0 to 8.0. When images were quantified using Image J software, the blue fluorescence intensity showed enhanced features along with reduced green fluorescence intensity (Fig. 2b).

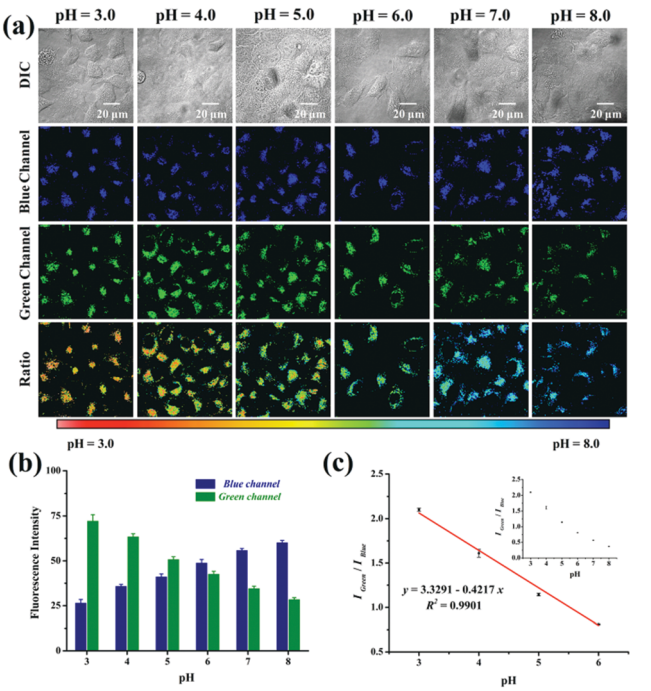

Fig. 2 (a) Two-photon fluorescence images of **Lyso-MPCB** (10 μM) in MCF-7 cells with various pH values (pH = 3.0–8.0): blue channel, λ_{em} range: 400–420 nm; green channel, λ_{em} range: 465–485 nm. Two-photon excitation wavelength: λ_{ex} = 760 nm. Ratio images represent the ratio of dual-channel intensity (I_{green}/I_{blue}). (b) Quantified relative fluorescence intensity of a certain pH was obtained employing Image J software and presented as mean ± SD, with n = 3. (c) The linear relationship of ratio (I_{green}/I_{blue}) *vs.* pH (pH = 3.0–6.0); inset: the dot plot of ratio (I_{green}/I_{blue}) *vs.* pH (pH = 3.0–8.0).

The fluorescence intensity ratio (I_{green}/I_{blue}) in cells also exhibited a good linear calibration curve to pH (pH = 3.0–6.0, Fig. 2c). It is just within the scope of the lysosomal pH value, which can help us to analyze the pH changes of lysosomes quantitatively. Taken together, **Lyso-MPCB** showed a wonderful capability for monitoring lysosomal pH value changes quantitatively.

Considering that the microenvironmental pH of cells would fluctuate during the autophagy process, we monitored the real-time changes of the lysosomal pH values with **Lyso-MPCB** in this lysosomes-related physiological pathway. The autophagy process here was stimulated under starvation conditions. In the beginning, the MCF-7 cells, co-stained with **Lyso-MPCB** (10 μM) were cultured in a medium without nutrients, Hank's Balanced Salt Solution (HBSS).[16] Then, the TP fluorescence images in the blue and green channel, including the ratio image analysis, were all acquired within 4 hours (Fig. 3a). In the first 1 hour, the fluorescence intensities both in the blue and green channels displayed no obvious change, as well as the ratio analysis. In particular, we chose a single cell in the red dashed box as the representative case for observing the variations of parameters within 4 hours. In the later 3 hours, the distribution range of the pseudocolor gradually became larger in the single cell. Moreover, the average level of pseudocolor also became deeper. These results demonstrated that the lysosomes in this cell were migrated step by step and the pH values in the lysosomal regions were decreased continuously in the later 3 h. In addition, the western blotting results (as shown in Fig. S8 (ESI†) and Fig. 3b, blue line) supplied accurate evidence that the membrane fusion procedure between the lysosomes and autophagosomes occurred after incubating cells with HBSS for 1 hour, which was in conformity with the TEM results in our reported work.[8b] Moreover, the specific pH values at different times of autophagy can be calculated intuitively and accurately, and the value was reduced from 5.2 to 4.6 (Fig. 3b, red line) in accordance with the analysis of Fig. 3a. Correspondingly, the pH values remained almost constant both under "rich-nutrient" conditions (Fig. S9 (ESI†) and Fig. 3b, orange line) and autophagy-inhibited conditions (HBSS with 3-methyladenine (3-MA) for inhibiting autophagy) (Fig. S10 (ESI†) and Fig. 3b, green line). These consequences demonstrated that **Lyso-MPCB** can be utilized as an available TP fluorescent probe for visualizing the autophagy process in real-time *via* quantifying the undulation of pH values with ratio signals.

In summary, a novel ratiometric TP fluorescent probe (**Lyso-MPCB**) was developed for detecting lysosomal pH changes. The probe displayed a dual-color response to pH with high sensitivity and selectivity, and the ratio values of the fluorescence intensities at 475 nm and 410 nm showed a great linear relationship with pH changes in solution as well as in living cells. More importantly, **Lyso-MPCB** can be used as an effective ratiometric fluorescence imaging tool for real-time visualization of autophagy by monitoring the lysosomal pH fluctuation.

This work was supported by the National Natural Science Foundation of China (21778001 and 21372005), the Natural Science Foundation of Anhui Province (1608085MB39 and 1808085MB47) and the Open fund for Discipline Construction

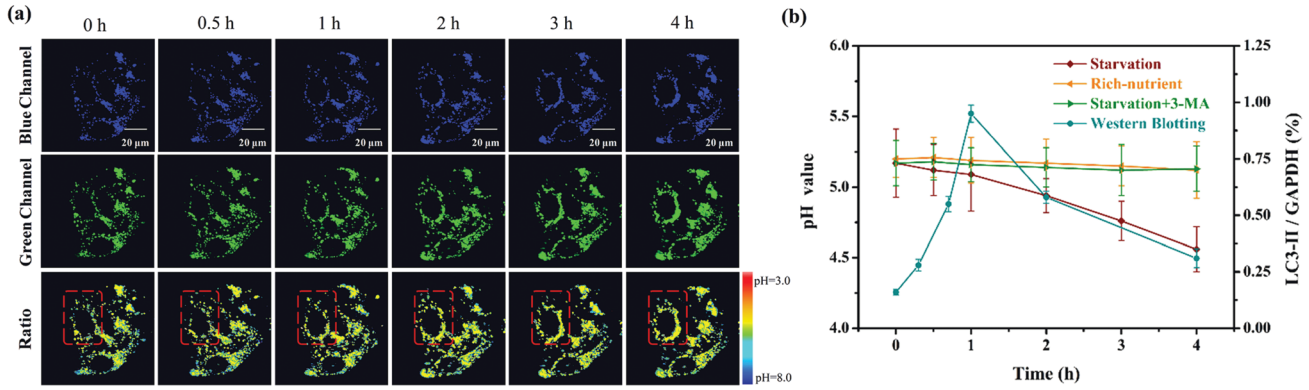

Fig. 3 Real-time visualization of autophagy using **Lyso-MPCB** in MCF-7 cells and relative western blotting study. (a) TP fluorescence dual-channel imaging of **Lyso-MPCB** in MCF-7 cells which were cultured under starvation conditions (medium of HBSS without bovine serum for inducing cell autophagy). Cells were incubated with **Lyso-MPCB** (10 μM) for 30 min before imaging. Blue channel λ_{em} range: 400–420 nm, green channel λ_{em} range: 465–485 nm, two-photon excitation wavelength: λ_{ex} = 760 nm, ratio images represent the ratio of dual-channel intensity (I_{green}/I_{blue}). (b) Quantified pH values of a certain time (0–4 h) under different conditions (Starvation, Rich-nutrient and Starvation + 3-MA) along with expression results of LC3-II and GAPDH under starvation conditions.

in Institute of Physical Science and Information Technology of Anhui University.

Conflicts of interest

There are no conflicts to declare.

Notes and references

1 (*a*) J. J. Lum, R. J. DeBerardinis and C. B. Thompson, *Nat. Rev. Mol. Cell Biol.*, 2005, **6**, 439–448; (*b*) N. J. Dolman, K. M. Chambers, B. Mandavilli, R. H. Batchelor and M. S. Janes, *Autophagy*, 2013, **9**, 1653–1662.
2 (*a*) N. Sun, D. Malide, L. Jie, I. I. Rovira, C. A. Combs and T. Finkel, *Nat. Protoc.*, 2017, **12**, 1576–1586; (*b*) Y. X. Lin, Y. Wang and H. Wang, *Small*, 2017, **13**, 1700996; (*c*) A. Kuma, M. Matsui and N. Mizushima, *Autophagy*, 2007, **3**, 323–328.
3 J. J. Diao, R. Liu, Y. G. Rong, M. L. Zhao, J. Zhang, Y. Lai, Q. J. Zhou, L. M. Wilz, J. X. Li, S. Vivona, R. A. Pfuetzner, A. T. Brunger and Q. Zhong, *Nature*, 2015, **520**, 563–566.
4 (*a*) M. B. Azad, Y. Chen, E. S. Henson, J. Cizeau, E. McmillanWard, S. J. Israels and S. B. Gibson, *Autophagy*, 2008, **4**, 195–204; (*b*) G. Maulucci, M. Chiarpotto, M. Papi, D. Samengo, G. Pani and M. DeSpirito, *Autophagy*, 2015, **11**, 1905–1916.
5 (*a*) Y. K. Yue, F. J. Huo, S. Y. Lee, C. X. Yin and J. Yoon, *Analyst*, 2017, **142**, 30–41; (*b*) H. J. Kim, C. H. Heo and H. M. Kim, *J. Am. Chem. Soc.*, 2013, **135**, 17969–17977; (*c*) L. L. Wu, Y. Wang, T. D. James, N. Q. Jia and C. S. Huang, *Chem. Commun.*, 2018, **54**, 5518–5521; (*d*) Y. B. Zhang, S. A. Xia, M. X. Fang, W. F. Mazi, Y. B. Zeng, T. Johnston, A. Pap, R. L. Luck and H. Y. Liu, *Chem. Commun.*, 2018, **54**, 7625–7628.
6 (*a*) M. H. Lee, N. Park, C. Yi, J. H. Han, J. H. Hong, K. P. Kim, D. H. Kang, J. L. Sessler, C. Kang and J. S. Kim, *J. Am. Chem. Soc.*, 2014, **136**, 14136–14142; (*b*) H. Iwashita, S. Torii, N. Nagahora, M. Ishiyama, K. Shioji, K. Sasamoto, S. Shimizu and K. Okuma, *ACS Chem. Biol.*, 2017, **12**, 2546–2551; (*c*) L. Q. Niu, J. Huang, Z. J. Yan, Y. H. Men, Y. Luo, X. M. Zhou, J. M. Wang and J. H. Wang, *Spectrochim. Acta, Part A*, 2019, **207**, 123–131; (*d*) Y. Liu, J. Zhou, L. J. Wang, X. X. Hu, X. J. Liu, M. R. Liu, Z. H. Cao, D. H. Shangguan and W. H. Tan, *J. Am. Chem. Soc.*, 2016, **138**, 12368–12374; (*e*) Y. C. Liu, L. L. Teng, L. L. Chen, H. C. Ma, H. W. Liu and X. B. Zhang, *Chem. Sci.*, 2018, **9**, 5347–5353; (*f*) H. Iwashita, H. T. Sakurai, N. Nagahora, M. Ishiyama, K. Shioji, K. Sasamoto, K. Okuma, S. Shimizu and Y. Ueno, *FEBS Lett.*, 2018, **592**, 559–567.
7 (*a*) M. H. Lee, J. S. Kim and J. L. Sessler, *Chem. Soc. Rev.*, 2015, **44**, 4185–4191; (*b*) M. A. Haidekker and E. A. Theodorakis, *J. Mater. Chem. C*, 2016, **4**, 2707–2718.
8 (*a*) L. L. Hou, P. Ning, Y. Feng, Y. Q. Ding, L. Bai, L. Li, H. Z. Yu and X. M. Meng, *Anal. Chem.*, 2018, **90**, 7122–7126; (*b*) J. C. Jiang, X. H. Tian, C. Z. Xu, S. X. Wang, Y. Feng, M. Chen, H. Z. Yu, M. Z. Zhu and X. M. Meng, *Chem. Commun.*, 2017, **53**, 3645–3648; (*c*) W. J. Wang, P. Ning, Q. Wang, W. Zhang, J. Jiang, Y. Feng and X. M. Meng, *J. Mater. Chem. B*, 2018, **6**, 1764–1770.
9 (*a*) Y. Wen, W. J. Zhang, T. Liu, F. J. Huo and C. X. Yin, *Anal. Chem.*, 2017, **89**, 11869–11874; (*b*) Q. Q. Wan, S. M. Chen, W. Shi, L. H. Li and H. M. Ma, *Angew. Chem., Int. Ed.*, 2014, **53**, 10916–10920.
10 (*a*) X. Luo, H. T. Yang, H. L. Wang, Z. W. Ye, Z. N. Zhou, L. Y. Gu, J. Q. Chen, Y. Xiao, X. W. Liang, X. H. Qian and Y. Y. Yang, *Anal. Chem.*, 2018, **90**, 5803–5809; (*b*) D. Yoshihara, T. Noguchi, B. Roy, J. Sakamoto, T. Yamamoto and S. Shinkai, *Chem. – Eur. J.*, 2017, **23**, 17663–17666; (*c*) M. J. Chang, K. Kim, K. S. Park, J. S. Kang, C. S. Lim, H. M. Kim, C. Kang and M. H. Lee, *Chem. Commun.*, 2018, **54**, 13531–13534.
11 (*a*) J. T. Hou, W. X. Ren, K. Li, J. Seo, A. Sharma, Q. Yu and J. S. Kim, *Chem. Soc. Rev.*, 2017, **46**, 2076–2090; (*b*) F. Galindo, M. I. Burguete, L. Vigara, S. V. Luis, N. Kabir, J. Gavrilovic and D. A. Russell, *Angew. Chem., Int. Ed.*, 2005, **44**, 6504–6508.
12 G. P. Li, D. J. Zhu, L. Xue and H. Jiang, *Org. Lett.*, 2013, **15**, 5020–5023.
13 (*a*) A. V. Marenich, C. J. Cramer and D. G. Truhlar, *J. Phys. Chem. B*, 2009, **113**, 6378–6396; (*b*) L. Yuan, W. Y. Lin, J. Z. Song and Y. T. Yang, *Chem. Commun.*, 2011, **47**, 12691–12693.
14 C. Xu and W. W. Webb, *J. Opt. Soc. Am. B*, 1996, **13**, 481–491.
15 (*a*) Z. X. Liu, X. Zhou, Y. Miao, Y. Hu, N. Y. Kwon, X. Wu and J. Y. Yoon, *Angew. Chem., Int. Ed.*, 2017, **56**, 5812–5816; (*b*) L. P. Qiu, T. Zhang, J. H. Jiang, C. C. Wu, G. Z. Zhu, M. X. You, X. G. Chen, L. Q. Zhang, C. Cui, R. Q. Yu and W. H. Tan, *J. Am. Chem. Soc.*, 2014, **136**, 13090–13093.
16 E. Desideri, G. Filomeni and M. R. Ciriolo, *Autophagy*, 2012, **8**, 1769–1781.